Microfluidic Array for Real-Time and High Content Live-Cell Imaging of Human and Rodent Pancreatic Islets

Mohammad Nourmohammadzadeh,[ab] Yuan Xing,[ab] Jin Wuk Lee,[c] Matthew A. Bochenek,[ab] Joshua E. Mendoza-Elias,[ab] James J. McGarrigle,[a] Enza Marchese,[a] David T. Eddington,[b] José Oberholzer,*[ab] and Yong Wang*[ab]

Design principle and device configuration

The array device utilizes the hydrodynamic trapping principle to immobilize individual islets in traps. The final design of the device contains an array consisting of 2 rows and 10 columns. In each column, there are 15 trapping sites that amounts to a total of 300 traps. The trapping site design is a U-cup shaped pocket, superimposed onto a loop channel that is used for delivery of fluids and islets. The U-cup pocket is 250 µm in diameter and 275 µm in depth. There is a cross-flow channel at the apex of the U-cup pocket with a subsequent reduction in the width to 45 µm. These design parameters allow for the capture of approximately 95% of the islet cell population. Additionally, the width and height of the loop channels are 300 µm and 250 µm, respectively, which allow the islets to move freely along the channel without clogging. Based on the flow resistant difference between the U-cup and the loop channel, the flow encountered less resistance in the unoccupied U-cup. When flow carries an islet to the junction between the U-cup and the loop channel, an islet becomes trapped in the U-cup due to the flow resistant difference between the U-cup and the loop channel. The trapped islet results in increased resistance in the U-cup and the flow is then redirected into the loop channel. This flow carries subsequent islets towards the next empty trap, iterating the trapping downstream throughout the device.

Calculation of pressure drop for designing microchannel geometry

In order to optimize the trapping efficacy for islets, flow resistance of the U-cup and the loop channel was calculated using the Dary-Weisbach equation, which was further modified by Poiseuille's Law for a rectangular channel. The value of the Darcy friction factor f is related to the aspect ratio of a channel and Reynolds number, in a product expressed as $C(\alpha) = f \times Re$. After simplification, the following expression was used for resistance:

$$\Delta P = \frac{C(\alpha)}{32} \times \frac{\mu L Q P^2}{A^3} \quad (\mathbf{1})$$

Where α is aspect ratio, L is length of the channel, A is cross sectional area, Q is flow rate, and P is channel perimeter.

In the absence of trapped islets, the U-cup pocket and the loop channel share the same pressure input. If the resistance for the U-cup pocket is less than that of the loop channel, then the volumetric flow will be greater, allowing an islet to be directed into the U-cup pocket.

$$\frac{Q_1}{Q_2} = \frac{C_2(\alpha_2)}{C_1(\alpha_1)} \times \frac{L_2}{L_1} \times \left(\frac{P_2}{P_1}\right)^2 \times \left(\frac{A_1}{A_2}\right)^2 = \frac{C_2(\alpha_2)}{C_1(\alpha_1)} \times \frac{L_2}{L_1} \times \left(\frac{W_2+H}{W_1+H}\right)^2 \times \left(\frac{W_1}{W_2}\right)^2 > 1 \quad (\mathbf{2})$$

Where A = W x H; H is the height of the channels, and W is the width, L_1 = the length of the cross-flow channel, L_2 = the length of the loop channel, W_1 = the width of the cross-flow channel, W_2 = the width of the loop channel.

L_2/L_1 and W_2/W_1 are important design parameters that could determine the capture efficiency when the channel height is constant. To achieve higher capture efficiency, it is desirable to minimize the gap for capturing majority of islet population in the cross channel and maximize the width of the main channel as this avoids clogging; however, there are some constraints in determining these dimensions. The width of the U-cup cross-flow channel (W_1) should be smaller than the diameter of the islets in order to be an effective trap. On the other hand, the width of the loop channel (W_2) and the channel height (H) should be larger than islet diameter to allow for continuous flow without clogging. H should also be short enough to minimize leakage around the immobilized islet, and prevent multiple islets becoming trapped in a single trap.

Device fabrication

The array device was designed in AutoCAD and printed on high resolution (16,000 dpi) transparency film (Fineline Imaging, CO). The transparency was used as a photomask to selectively crosslink prespun photoresist to a desired thickness on a silicon wafer. Briefly, SU-8 2150 photoresist (Microchem, MA) was spun to achieve a thickness of 250

μm for the channel, in accordance to the manufacturer's protocol using precision spinner (Laurel Technology, PA). Following placement of the photomask, the photoresist was then exposed to UV light to polymerize and transfer the pattern to the SU-8. Finally, uncross-linked regions of photoresist were removed by washing the wafer in SU-8 developer solution. The PDMS was made by mixing 10:1 mass ratio of PDMS prepolymer to curing agent (Sylgard 184 kit, Dow Corning). Once the SU-8 negative mold master was fabricated, PDMS was poured onto the master to generate a positive mold at the desired thickness. The PDMS mixture was cured for 2 hours at 80ºC. Next, a cork-borer (gauge 11) was used to puncture inlet and outlet holes for the inlet and outlet ports. After fabrication of the PDMS component was completed, the device was assembled. The PDMS component was first cleaned with scotch tape. Then, PDMS component was bonded to thin coverslip (60 x 24 mm and 0.13 mm in thickness) after surface exposure to oxygen plasma and annealed on a hotplate at 80ºC for 1 hour while pressed with a 1 kg weight.

Human islet isolation

The islet isolation, purification, and culture procedures were performed as previously described. Briefly, the pancreata were first trimmed and distended with collagenase and then digested using a modified Ricordi semi-automatic method. Post-digestion, islets were purified using UIC-UB gradient in a Cobe 2991 cell separator (Cobe 2991, Cobe, CO) and subsequently cultured in CMRL1066 culture media (Mediatech, VA) at 37°C supplemented with insulin-transferrin-selenium (ITS; Invitrogen, CA), Sodium bicarbonate (Sigma, MO), Hepes, Human Albumin (Grifols, CA) and Ciprofloxacin (Hospira INC., USA).

Mouse islet isolation

Mouse islet isolations were performed as previously described. Briefly, 0.375 mg/mL Collagenase P (Roche, Applied Science, IN) was dissolved in HBSS (Mediatech Inc. VA), and injected via the bile duct for pancreatic distention. After excision, the pancreata were digested in 15 mL conical tubes at 37**°**C for 11 min, gently shaken, and washed twice with HBSS. Discontinuous Ficoll density gradients (Mediatech Inc., VA) were used for islet purification. Islets were then cultured in RPMI 1640 containing 10 % FBS at 37°C.

Real-time fluorescence imaging

Imaging experiments were performed according to our previously established protocol. In brief, isolated islets were incubated with 5 μM Fura-2/AM (a calcium indicator, Molecular probes, CA) or 2.5 μM Rhodamine 123 (Rh123, a mitochondrial potentials indicator, Sigma, MO) in KRB2 for 30 min at 37°C. The islets were then introduced into the temperature-controlled microfluidic device by gravity through the inlet microchannel and mounted on an inverted epifluorescence microscope (Leica DMI 4000B). The loaded islets were then perifused by a continuous flow of KRB containing 2 mM glucose at 37°C (pH 7.4) for 10 min in order to washing out extra fluorescence dyes. KRB containing 25 mM of glucose and 30 mM KCl were administered to the islets by gravity flow for 20 min and 10 min, respectively, and were simultaneously observed with 10 x objectives assisted by a computer-controlled motorized stage. Dual-wavelength Fura-2 was excited ratiometrically at 340 and 380 nm, and changes in $[Ca^{2+}]$ are expressed as F_{340}/F_{380} (%). Rh123 is a lipophilic cation that partitions selectively into the negatively-charged mitochondrial membrane. Hyperpolarization of the mitochondrial membrane causes an uptake of Rh123 into the mitochondria and a decrease in fluorescence is observed due to intermolecular crowding and quenching. Rh123 is excited at 495 nm; excitation wavelengths were controlled by means of suitable excitation filters (Chroma Technology) mounted in a Lambda DG-4 wavelength switcher. Emission of Fura-2/AM and Rh123 fluorescence was filtered using a Fura2/FITC polychroic beamsplitter and double band emission filter (Chroma Technology. Part number: 73.100bs). SimplePCI software (Hamamatsu Corp) was used for imaging acquisition and analysis. These images were collected with a high-speed, high-resolution charge coupled camera (CCD, Retiga-SRV, Fast 1394, QImaging).

Computer simulation

To better understand the flow characteristics around the microfluidic traps and determine the optimal parameters for microfluidic channel design, a computational fluid dynamics (CFD) analysis was carried out using COMSOL 4.4 (COMSOL Multiphysics, Sweden). The fluid material inside the channel was water ($\rho = 1000\,\mathrm{kg/m^3}$) with a dynamic viscosity of $\eta = 0.001\,\mathrm{Pa}$, and an incompressible flow model was applied to the fluid. No slip conditions were imposed on the channel walls, and the input/output boundary condition was set by the fluid velocity of V_{in} =

$10\ \mu m\ S^{-1}$ and pressure of $P_{out} = 0$, respectively. The environmental temperature (T) was set at $293.15\ K$. The complete mesh consisted of 79,561 elements and error tolerance was set at 10^{-6}.
The COMSOL fluid-flow simulation results using a 2D model were depicted in SI Figure 1. The pressure profile in the microfluidic channel was shown in SI Figure 1A. It shows that the pressure decreased along the islet array, indicative of no significant counter flow. The velocity profile in the whole device presented in SI Figure 1B indicates that velocity pattern was periodically repeated and identical in each row and column. Since the islet array had 2 identical rows and each row contained 10 columns with 15 islet traps of fixed width and height, it was expected that flow velocity should be the same as the fluid flow entered the trapping area, as well as the loop channel.

A close-up view of the velocity pattern around the trapping area is shown in SI Figure 1C. Theoretically, close to the trapping area a particle may experience two stream flows: a partial stream flow (Q_1) directing particles into the trap site and a mainstream flow (Q_2) along the loop channel. If the Q_1/Q_2 ratio is in a proper range (>1), particles can be guided into the trapping sites and immobilized. When the trapping area was not occupied, there was a higher flow velocity at the cross-flow channel of the trapping area as expected. When the trapping area was occupied, flow velocity of the loop channel was increased resulting in moving particles into the next available trapping area. For comparison, a simulation of the velocity streamline was also conducted. As shown in the insert of SI Figure 1C, it was observed that much of the fluid flowed into the cross-flow channel, which indicated partially diverted flow into the trapping area. This would allow particles to flow toward the trapping sites due to the hydrodynamic force. When a particle occupied the trapping area, it increased flow resistance that allowed flow to bypass the trapping area and directed remaining islets into the loop channel.

We further verified flow dynamics prior to trapping site and post trapping site in the array (SI Figure 2A and SIV2) with 2D COMSOL simulation for flow velocity measurement. When the trapping sites were occupied by a particle, P_1 (the prior to trapping site) and P_2 (post trapping site) had almost identical flow velocity (SI Figures 2B), and the difference between two profile is the flow that goes through cross channel in presence of particles. This indicates that even though the trapping sites are occupied by particle, a portion of flow goes through the cross channels which results in an effective stimulation. While when the trapping sites were empty, the majority of flow passed through the cross-flow channel rather than down the loop channel reflected as shown in post trapping site designated as P_4 (SI Figures 2B).

Islet loading, stimulation, and retrieval

Prior to islet loading, 100% ethanol was passed through the microfluidic array for 5 min to prevent potential bubble formation. The array was then rinsed with Krebs-Ringer buffer (KRB) containing 2 mM glucose (KRB2) for 2 min while positioned on a glass heating stage at 37°C. In order to achieve a high trapping efficacy with minimal shear force exerted on the islets, both islets and solutions containing insulin secretagogues were delivered into the device using a hydrostatic pressure-driven method (SI Figures 3A-3C and SIV1). Briefly, a 1 mL pipette tip was inserted into the inlet and the tip filled with KRB2 up to 20 mm in height (20 mm higher than the outlet), while waste tubing was clamped and placed −2 cm with respect to the plane of the chip. Islets were transferred to the loading tip via a 20 µl pipette. After loading the islets, the waste tubing was unplugged so that the solution flowed to the waste as the islet was drawn into the chip. The islets continued to move slowly into the chip by gravity. Using this method, 100 islets were arrayed in less than 60 s. For stimulation, the 1 mL pipette tip was refilled with insulin secretagogues and delivered to the islets by gravity. Post stimulation, loaded islet cells can be collected for further analysis by reversal of the flow through the outlet (SI Figure 3D).

Confocal imaging and data analysis

Islets were stained with CellTracker Green CMFDA for live cells (Invitrogen, USA), and propidium iodide (PI, Invitrogen, USA) for dead cells. Briefly, islets were incubated in culture medium containing $10\ \mu M$ CellTracker Green CMFDA for 30 min. The medium was then replaced with serum-free medium supplemented with $1\ \mu l/ml$ PI $(1\ mg/ml)$ for an additional 10 min prior to analysis by confocal microscopy (Zeiss LSM 710, Oberkochen, Germany). CellTracker Green CMFDA was excited at 488 nm and emitted at 525 nm, while PI was excited at 561 nm and emitted at 595 nm. Images were acquired using a 20 x objective. The ZEN software utility package was used for image capture and processing.

Fluid exchange efficiency

In order to make sure we achieved a uniform solution distribution and a fast rate of solution exchange in the array channel, a fluorescent intensity experiment using FITC was carried out (SI Figure 4 and SIV3).

The fluorescence intensity of perfused solutions measured over time across different regions inside the perifusion channel during the perifusion of DI water and fluorescein intensity of the solution was measured. The intensity values were area averages of three different scans. The intensity changes in the plots clearly illustrated the ability of the array device to completely exchange its stimulatory solution in approximately 10 sec and the fluorescence profiles of each location were identical (SI Figure 4C). The rate of solution exchange was significantly faster as a result of small channel size and volume in comparison to our previous chamber design, which required 3 min to fully exchange. This allows faster stimulation, shorter washing time, and improved resolution.

SI Figures and SI Videos

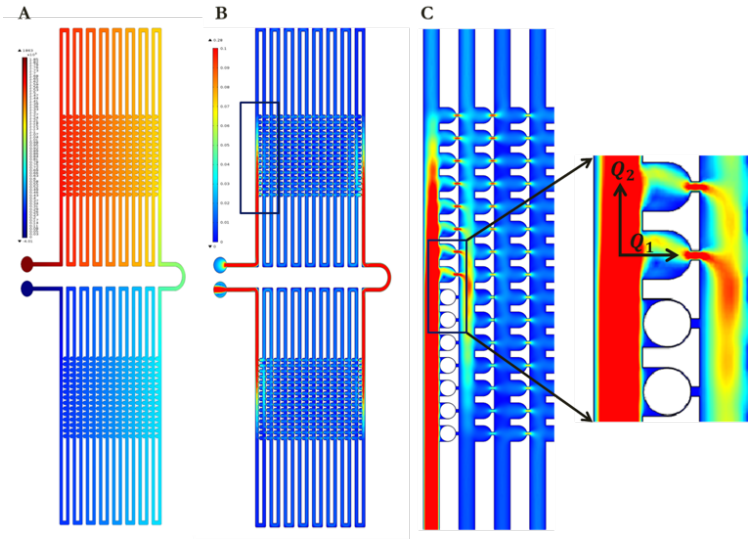

SI Figure 1. Computer simulation of flow dynamic. (A) Computer simulation of pressure profile. **(B)** Computer simulation of velocity profile. **(C)** Computer simulation of flow stream and velocity profile with and without particles trapping.

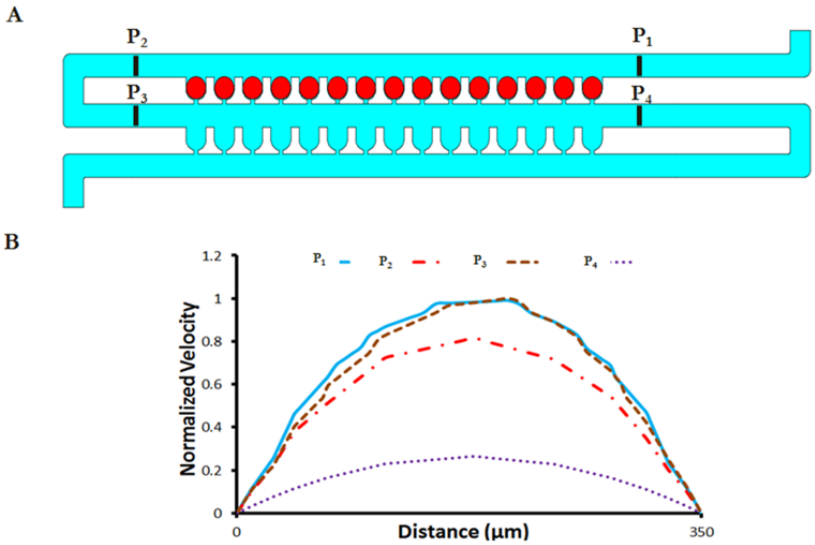

SI Figure 2. Computer simulation and experimental validation of flow dynamics. (A) Schematic of the microfluidic islet array. **(B)** Computer flow simulation for flow velocity in four different position across the channel.

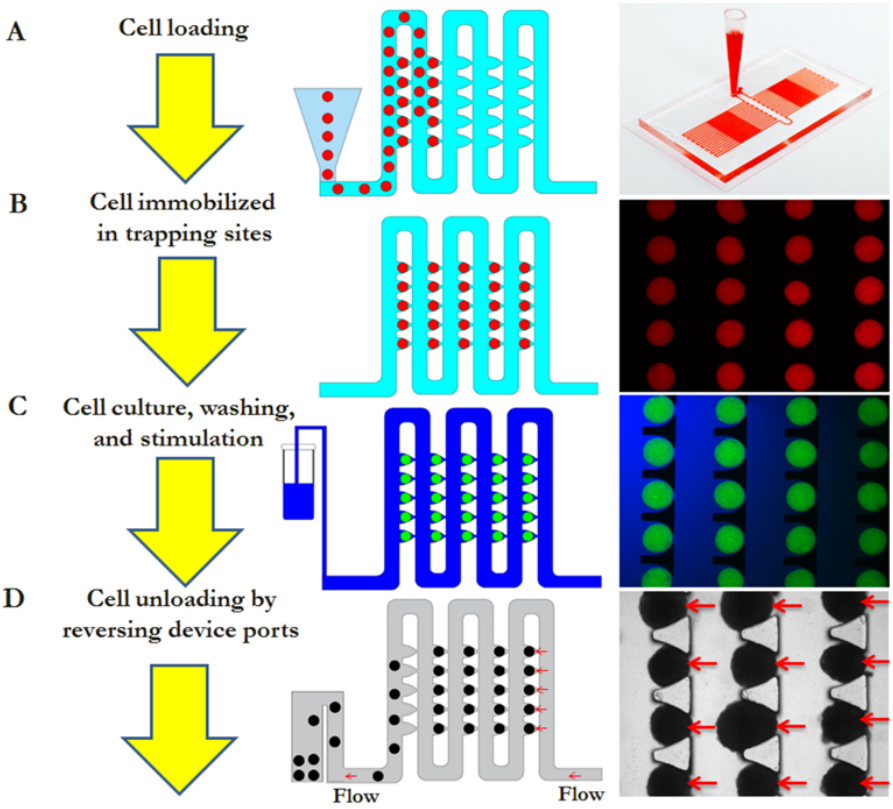

SI Figure 3. Islet loading, stimulation, and retrieval in the array. (A) Schematic of islet loading and a photo image of the islet array. **(B)** Schematic of islet trapping and trapped fluorescence beads (200-240 μm). **(C)** Schematic of islet stimulation and trapped fluorescence beads (200-240 μm). **(D)** Schematic of islet retrieval and human islets.

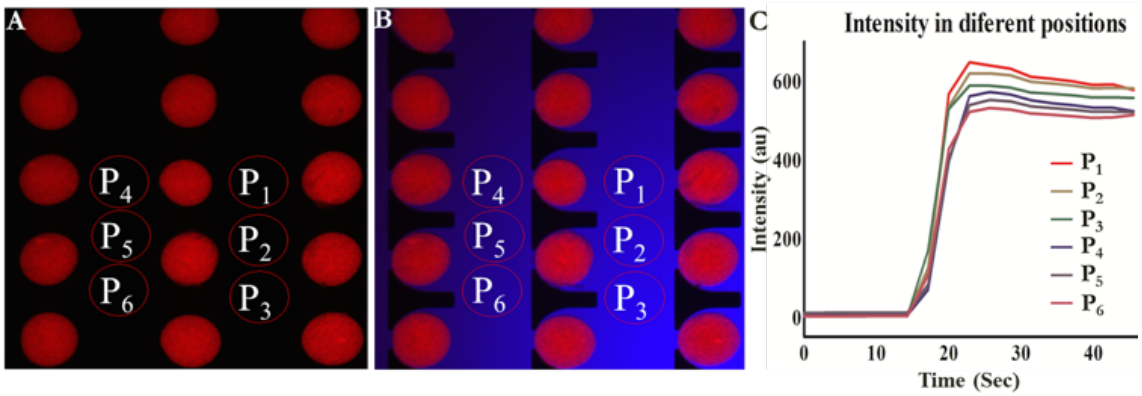

SI Figure 4. Fluid exchange efficiency. (A) The array loaded with fluorescence beads (200-240 µm). **(B)** The array loaded with fluorescence beads (200-240 µm) flushed with 2.5 µM FITC. **(C)** FITC intensity profiles at different locations in the array.

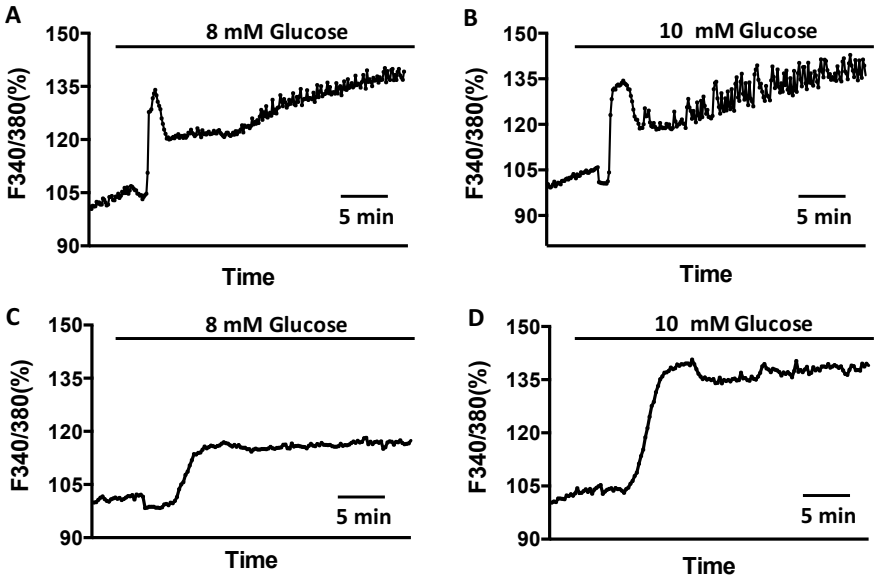

SI Figure 5. Intracellular Calcium profiles in response to varying glucose concentrations. (A) Representative of intracellular calcium profile of mouse islets in response to 8 mM glucose. **(B)** Representative of intracellular calcium profile of mouse islets in response to 10 mM glucose. **(C)** Representative of intracellular calcium profile of human islets in response to 8 mM glucose. **(D)** Representative of intracellular calcium profile of human islets in response to 10 mM glucose. N= 10-15 islets.

Video Legends:

Supplementary Video 1: Sequential trapping of islets in trapping sites.

Supplementary Video 2: Flow simulation and particle tracing in microfluidic array using COMSOL 4.4.

Supplementary Video 3: Fluid exchange studies over time across different regions inside the perifusion channel during the perifusion of DI water and fluorescein solutions.